Catalysis Letters Vol. 102, Nos. 3–4, August 2005 (© 2005)
DOI: 10.1007/s10562-005-5858-2

Novel precipitated iron Fischer–Tropsch catalysts with Fe_3O_4 coexisting with α-Fe_2O_3

Baoshan Wu, Lei Tian, Hongwei Xiang, Zhixin Zhang, and Yong-Wang Li*

State Key Laboratory of Coal Conversion, Institute of Coal Chemistry, Chinese Academy of Sciences, P.O. Box 165 Taiyuan 030001, People's Republic of China

Received 16 February 2005; accepted 19 April 2005

The present study was undertaken to investigate the catalytic behavior of an industrial iron catalyst ($Fe/Cu/K/SiO_2$) prepared from ferrous sulfate precursor for Fischer–Tropsch (FT) synthesis, in which different amount of Fe_3O_4 coexist with α-Fe_2O_3. The catalyst samples were characterized by BET, XRD, H_2-TPR and Mössbauer effect spectroscopy (MES). The FT synthesis performance of the catalysts were carried out in a fixed bed reactor (FBR) under reaction conditions of 250 °C, 1.5 MPa, 2.0 nL/g-cat/h, and $H_2/CO = 2/1$ for 200 h. The results from XRD and MES for the catalyst samples of pre- and post-reduction indicate that more iron carbides form in the catalysts that have lower Fe_3O_4 contents. H_2-TPR for the catalysts displays that Fe_3O_4 may facilitate the reduction of catalysts only when it was highly dispersed. FT reaction study in the FBR shows that the catalysts become more active with the decrease of Fe_3O_4 contents in the catalysts. However, the catalyst with certain amount of highly dispersed Fe_3O_4 exhibited high FT synthesis activity with CO conversion more than 75%. The catalyst also displayed much less olefins selectivity. A comparison of FTS performances of one of these catalysts with some known catalysts was also made in this paper.

KEY WORDS: Fischer–Tropsch synthesis; iron catalyst; fixed bed reactor; iron carbide; ferrous sulfate; slurry reactor.

1. Introduction

Fischer–Tropsch synthesis provides an alternative route for the production of clean transportation fuels and high molecular weight hydrocarbons via catalyzed CO hydrogenation. Much attention has been drawn both in FT synthesis catalytic studies and exploration of new technology for its industrial applications since its first development in German in 1923 [1–4]. Precipitated iron catalysts are often used for this reaction because of their low cost, flexible product distribution, and ability to use coal-derived synthesis gas with low H_2/CO ratios [5,6]. These catalysts need alkali (normally potassium) promotion to attain high activity and stability, accompanied by addition of copper for reduction promotion and addition of SiO_2 for structural promotion [7]. Extensive phase changes of the precipitated iron catalysts (initially α-Fe_2O_3 as the main phase) during activation and especially during FT reaction makes them the most complicated system among FT catalysts [8].

A great number of studies have been focused on the phase transformation and on catalytically active phase(s) for FT reaction over the iron catalysts. Fe carbides, Fe oxide (especially Fe_3O_4), Fe metal, or surface iron phases on Fe_3O_4 have been proposed to be the active species for FT reaction by different researchers [9–15]. The kinds and the relative abundances of these phases depend on the varied activation procedures and different reaction conditions [16,17].

Some recent investigations on active site for FT synthesis over precipitated iron catalysts by *in situ* technologies, such as IR [18], SSITKA [19], and Mössbauer spectroscopy (MES) [20] provided more information about active phases. FT-IR studies with a precipitated iron catalyst reduced by CO, or firstly H_2 then CO, showed that iron carbides on the reduced samples have high ability to CO dissociation [18]. These iron carbides have played an important role in enhancing the catalyst activity. SSITKA studies on the effect of activation method on Fe FT catalysts at site level by Goodwin *et al.* suggested that the active sites on Fe samples activated differently (using H_2, CO, or syngas, respectively) were identical. The active sites for CO hydrogenation on Fe catalysts proposed to be on a carburized Fe surfaces [19]. *In situ* MES study provided more evidence about relationship between the catalytic activity and the formation of iron carbides [20]. XANES and EXAFS studies on FT synthesis over iron catalysts promoted by K and Cu illustrated the phase transformation on the surfaces in details [21–23]. The results exhibited that FT reaction rate increased markedly during the initial stages of carburization. These studies suggested for the first time that hydrocarbon synthesis reactions became detectable only as Fe_3O_4 formed and rapidly converted to FeC_x, and that the surface areas of particles with Fe_3O_4 or FeC_x composition in near surface layers controlled FT reaction rates.

* To whom correspondence should be addressed.
E-mail: ywl@sxicc.ac.cn

Since Fe_3O_4 is supposed to be an important intermediate phase correlated with the formation of iron carbides from α-Fe_2O_3 and/or with high catalyst activity during pretreatment and FT synthesis, it is necessary to know the actual function of Fe_3O_4 from initial stage. The objective of present work is to prepare a new series of Fe/Cu/K/SiO_2 catalysts that derived from different oxidation states of iron, and to investigate the effect of initial Fe_3O_4 phase on the catalytic behaviors during the activation and the FT reaction. It is well known that nearly all the iron catalysts for FT synthesis studies are prepared from iron nitrate and have unique α-Fe_2O_3 phases before the reactions. In our previous works, active and stable Fe/Cu/K/SiO_2 catalysts containing certain amounts of sulfate for slurry FT synthesis were prepared from ferrous sulfate [24,25]. At present work, different ratio of Fe^{3+}/Fe (total) solutions that were derived from iron sulfate were used to prepare a series of FT synthesis catalysts in which different amount of Fe_3O_4 coexist with α-Fe_2O_3. Investigations were made on iron phase transformations and on resulting effects during catalyst activation and FT reaction in the paper.

2. Experimental

2.1. Catalysts

The group of catalysts was prepared referred to a patented method (Chinese Patent register No. 200410012503.7). Four mixed solutions of $FeSO_4 \cdot H_2O$ and copper nitrate with same Fe/Cu ratio, respectively, reacted with appropriate amounts of oxidizing agent (25%, 50%, 75% and 110% of the calculate dosage for completely oxygenation of Fe^{2+} to Fe^{3+}). The reactants were heated to eliminate the extra oxidizing agent. The permanganate titration was performed on the reactants samples to determine the ratios of Fe^{3+}/Fe^{2+} in those solutions [26]. And then the solutions were precipitated with sodium carbonate solutions, respectively. The filtrate cakes were washed by deionized water for several times to eliminate SO_4^{2-} and other impurities. The cakes were re-slurred and added with appropriate amount of K_2SiO_3 solution. After dried in air in an oven, the catalyst precursors were calcined at 350 °C for 5 h. Four catalysts prepared with 25%, 50%, 75% and 110% of oxidizing agent were labeled as FO25, FO50, FO75, and FO100. The compositions of the as-prepared catalysts were determined by atomic absorption spectroscopy on a TJA AtomScan16 absorption spectro-photometer.

2.2. Catalysts characterization

The BET surface area and pore volume of catalysts were determined by ASAP 2010 (Micromeritics Instrument Corporation) using N_2 adsorption at 77 K.

A Rigaku D/max RB X-ray diffractometer was used at 40 kV, 100 mA (Cu Kα radiation) for the XRD measurements.

Temperature programmed reduction (TPR) was operated on an equipment (with mixed gas of 5% H_2 in highly purified N_2 as reduction gas) to study the reduction behaviors of the catalysts. Consumption of H_2 was monitored by changes in the thermal conductivity (TCD) of the effluent gas stream.

Mössbauer spectroscopy (MES) experiments were carried out using a S-600 Mössbauer spectrometer (Austin Co.), equipped with dual ^{57}Co sources in a Pd martrix. All samples were investigated at the room temperature. All spectra have been analyzed by means of a least-squares fitting procedure that models the spectra as combinations of quadruple doubles and magnetic sextets based on Lorenzian line-shape profile.

A laboratory fixed bed reactor (1 cm I.D., stainless steel tube) was used for FT reaction tests. The catalysts were sieved to particles of 20–40 meshes. Five gram catalyst was, respectively, mounted in the reactor and was activated using synthesis gas with H_2/CO ratio of 2.0 under 260 °C, 0.25 MPa, and 1.0 nL/g-cat/h for 24 h. The synthesis gas was introduced through a series of purification columns to remove oxygen, sulfides, water, and carbonyls. Then it was quantified by a mass flowmeter before entering the reactor. The exit gas passed through a high temperature trap equipped under the reactor tube to accumulate waxes, and a cool trap to accumulate liquid products. The pressure was released and a wet-flow meter was used to quantify the tail gas. A stirred tank slurry reactor (STSR) was also used. The information about the reactor was described in detail elsewhere [24].

During the mass balance period (usually 24 h), the tail gas was analyzed on an off-line GC (SHIMADZU GC-9A) every 8 h. The wax was analyzed on GC (GC-920) using a fused silica capillary column. After separated into aqueous and organic phases, liquid products were analyzed, respectively, by GCs with different columns [27]. The total and individual atomic closures of carbon, hydrogen, and oxygen were calculated based on the analysis of all products collected. Atomic closures of $100 \pm 3\%$ were obtained for the mass balances.

3. Results and discussion

3.1. Catalyst

The nominal composition of the four catalysts is 100Fe/5Cu/3K/8SiO_2 (on mass basis). The actual compositions of FO75 and FO100 were determined by ICP-AES as 100Fe/5.0Cu/2.2K/6.9SiO_2 and 100Fe/4.9Cu/2.8K/7.5SiO_2, respectively, which are in agreement with the designed composition. Main impurities in the as-prepared catalysts such as sulfate and sodium were also determined. The results are listed in table 1. Sulfate

Table 1
Preparation parameters and microstructure of the catalysts

Cat. number	Ratio of $Fe^{3+}/(Fe^{2+}+Fe^{3+})$ in initial iron precursors (mol/mol)	Content of main impurities (wt%)		Surface area (m^2/g)	Pore volume (cm^3/g)
		SO_4^{2-}	Na^+		
FO25	0.26	0.032		96	0.25
FO50	0.51	0.020		59	0.22
FO75[a]	0.78	0.036	0.38	139	0.38
FO100[b]	>0.99	0.024	0.24	153	0.40

[a]100Fe/5.0Cu/2.6K/6.9SiO_2.
[b]100Fe/4.9Cu/2.8K/7.5SiO_2.

concentrations of the four catalysts are within the range of 200–360 ppm, which are comparable with the catalyst we described previously [24]. The sodium content of the catalyst FO75 and FO100 are 0.38 and 0.24 wt%, respectively. These impurities may have detectable influence on catalyst microstructure and its FTS performance even at very low levels (will discussed below).

The BET surface areas and pore volumes of the catalysts are also summarized in table 1. It can be seen that with the increase of initial oxidation degrees of iron, the surface area and pore volume of the catalysts increase remarkably except for FO50, which have the lowest surface area and smallest pore volume. FO100 has the very high surface area (153 m^2/g) that is nearly three times higher than that of FO50 (59 m^2/g). FO100 also possesses of large pore volume (0.40 cm^3/g). Considering that the four catalysts have the same binder content, some reasons are suggested for their differences in microstructures. One possible reason is that different iron hydrates were formed during the precipitation. They might produce varied pores that influence morphology of the as-prepared catalysts during the calcinations. It is generally accepted that the α-Fe_2O_3 phase in precipitated iron catalysts is obtained from the dehydration of FeOOH precursor during the calcinations [20,28]. Other hydrates such as $Fe(OH)_2$ and complex with mixed oxidation state of iron will lead to form phases such as Fe_3O_4 and γ-Fe_2O_3. Different amount of oxidizing agent used may be the other important factor. More oxidizing agent used is responsible for higher surface area.

3.2. X-ray diffraction study

Figure 1 is the XRD patterns of the catalysts after calcination at 350 °C. As mentioned above, the XRD patterns of four catalysts are obviously different. The major Fe phases of catalyst FO25, FO75, and FO100 were found to be α-Fe_2O_3 (hematite), while that of FO50 was Fe_3O_4 (magnetite). There are certain amounts of Fe_3O_4 species in FO25 and FO75 because of their incomplete oxidation of iron before co-precipitation. Furthermore, with the increase of oxidation degrees of iron, the peaks of incomplete oxide Fe_3O_4 become weak, while the peaks of α-Fe_2O_3 become obviously strong. FO50 is an exceptional. Other studies have proved that when the ratio of Fe^{3+}/Fe^{2+} is close to 1.0 in the solution before precipitation, pure magnetite is obtained [29].

The XRD patterns of the catalyst samples after pretreatment and after 200 h of FT reaction are shown in figures 2 and 3, respectively. The pretreatment condition was exactly the same with that in FT synthesis (260 °C, 1.5 MPa, 2.0 nL/g-cat/h, and $H_2/CO = 2.0$). The patterns of the catalyst samples after pretreatment

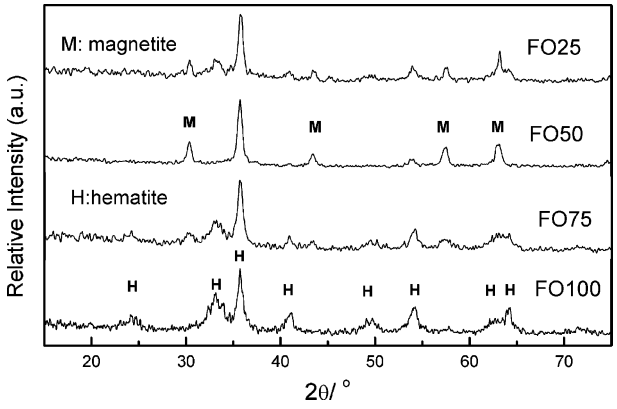

Figure 1. XRD patterns from the catalysts after calcination (350 °C).

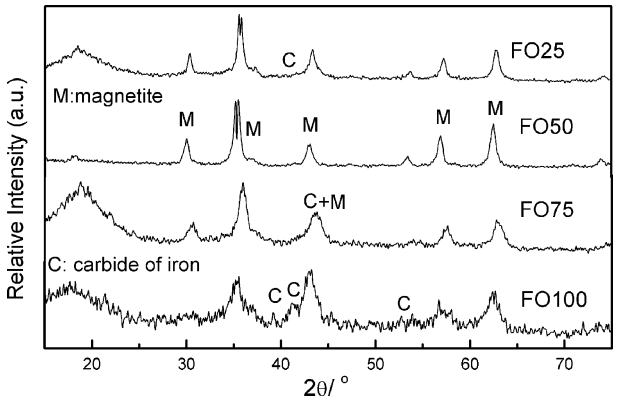

Figure 2. XRD patterns from the catalysts after pretreatment for 24 h.

(figure 3) have the main peaks at about 30°, 35.5°, 43.5°, 57.5°, and 63°, all of which are characteristic of Fe_3O_4 [19]. The dispersion of Fe_3O_4 phase increases follows the sequence as FO50, FO25, FO75, and FO100. The patterns also show some peaks of iron carbides at 39.5–44° in the samples, except for FO50, which does not show obvious phase changes after pretreatment. The peaks of iron carbides waxes increase in order of FO25, FO75, and FO100, indicating that more iron carbides were formed on the catalyst with high dispersion of iron oxides. The XRD patterns of the samples from catalysts after 200 h of FT reaction (figure 3) display somewhat similar variation trend to those after pretreatment. The amounts of iron carbide in the sample increase following the order of FO50, FO25, FO75, and FO100. These iron carbide peaks are neither sharp, nor having strong intensity, indicating that they are still highly dispersed in the catalysts. Compared with corresponding XRD patterns after pretreatment, the peaks of magnetite after FT reactions become sharper and have stronger intensity. It suggests that the contents of magnetite increase during FT reactions. The result may be ascribed to re-oxidation of iron carbides by water formation in FT synthesis. Water in reaction products sometimes serves as the oxidizing agent [30]. Sharp peaks of magnetite in XRD indicate that small particles congregate to large crystals during FT reactions.

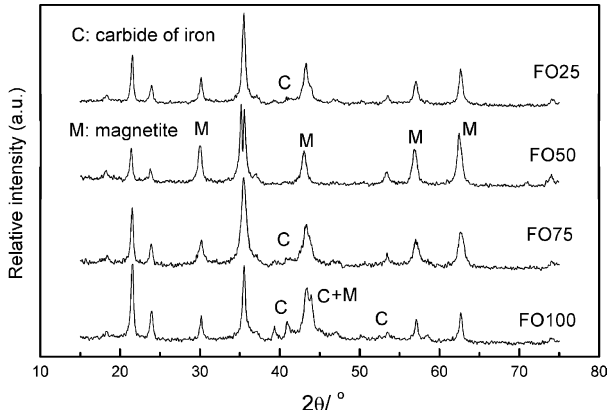

Figure 3. XRD patterns from the catalysts after reactions for 200 h.

3.3. Mössbauer spectroscopy study

Table 2 shows the phase composition for the catalysts in calcined state, and for the catalysts after pretreatment and after 200 h of FT reactions by MES analysis. The detected iron phases in as-prepared catalysts including α-Fe_2O_3, Fe_3O_4, Fe^{3+} (SPM) and partly γ-Fe_2O_3. Super paramagnetic (SPM) refers to iron phases located in small particles with diameter less than 13.5 nm [31]. These iron phases cannot be well identified at room temperature. The percentage of α-Fe_2O_3 phase in as-prepared catalysts increase following the sequence of FO50, FO25, FO75, and FO100, while the percentage of Fe_3O_4 decreases in a reverse way. The amounts of Fe^{3+} (SPM) increase following the sequence of FO50, FO25, FO75, and FO100, indicating that the particle size of the catalysts decreases and the dispersion of iron phase increase. The results are consistent with what were found in the XRD experiments. Nevertheless, there are some different results getting from the two characterization methods. FO100 shows the existence of certain amount of Fe_3O_4 (around 15%) in Mössbauer spectroscopy, while no Fe_3O_4 signals were detected in XRD.

From table 2, it can be seen that initial iron phase will determine their final phases after pretreatment and after FT reaction. FO50 shows highest percentage of Fe_3O_4 (85.9% in total Fe phase) in its calcined state. Fe_3O_4 kept as the dominant phase in its activated state and in the catalyst after FT reaction. Iron carbide was difficult to form on this catalyst. On the other hand, FO100 shows the least percentage of Fe_3O_4 (15.8% in total Fe phase) in its calcined state. About 58.0% of iron exists as iron carbide in its activated state. The amounts of Fe^{2+} (SPM, from iron carbides and/or Fe_3O_4) in activated catalyst samples increase following the sequence of FO50, FO25, FO75, and FO100. It is assumed that activation and carbonization are easier to take place on highly dispersed iron phases.

Table 2
MES assignment for the catalysts samples at room temperature

Iron phase assignment	Fe% before reaction				Fe% after pretreatment				Fe% after FT reaction			
	FO25	FO50	FO75	FO100	FO25	FO50	FO75	FO100	FO25	FO50	FO75	FO100
$\alpha-Fe_2O_3$	44.8	8.5	46.1	62.1								
Fe_3O_4	43.4	85.9	35.4	15.8	49.9	85.6	33.4	15.4	53.8	84.8	49.3	34.4
Spm (Fe^{3+})	11.8	3.5	18.5	22.1								
Spm (Fe^{2+})					20.3	1.2	24.4	26.6	7.9	4.8	17.5	13.0
Fe_xC					29.8	13.2	42.0	58.0	38.3	10.4	33.2	52.6
$\gamma-Fe_2O_3$		2.1										

3.4. Temperature programmed reduction study

Figure 4 shows the H_2-TPR profiles of the catalysts in calcined state. All the catalysts display three visible reduction peaks, labeled as A, B, and C, but their H_2 consumption profiles are quite different. In the cases of FO75 and FO100, the first two peaks (A + B in figure 4) corresponding to the transformations of $CuO \rightarrow Cu$ and α-$Fe_2O_3 \rightarrow Fe_3O_4$ are overlap. This always happened in H_2-TPR experiments for Fe/Cu/K catalysts, whether they have binders or not [32,33]. The reason is that CuO promoter facilitates the reduction of α-Fe_2O_3 when the two phases are well mixed, resulting in the reduction of α-Fe_2O_3 appears at much lower temperature. For the catalyst FO25 and FO50, the first set of shoulder peaks A can be identified to be the reduction of $CuO \rightarrow Cu$, according to their heights corresponding to theoretical values based on copper contents of the catalysts. The second peak B for FO50 is separated from A and appears at much higher temperature, indicating that copper oxide was not well mixed with iron oxide in FO50, therefore it is not able to promote the reduction of iron oxide at all. The last set of peaks C for the four catalysts display similar profiles, assigning to the transformation of $Fe_3O_4 \rightarrow$ α-Fe. Fe_3O_4 begins to reduce less than 400 °C for FO75, while it begins at 420 °C for FO25.

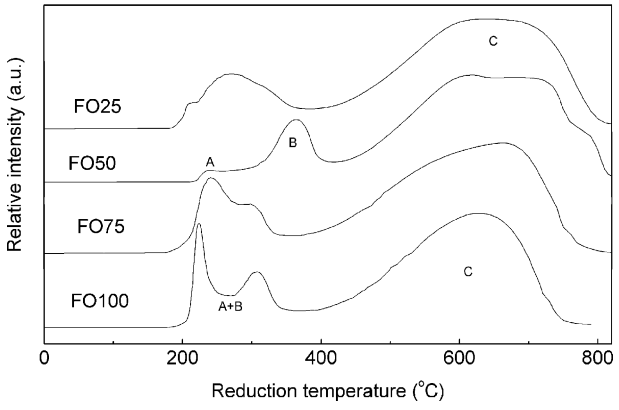

Figure 4. H_2-TPR results of the catalysts.

Combined with the results getting from BET, XRD, and MES, H_2-TPR demonstrates that highly dispersed α-Fe_2O_3 phase in FO75 and FO100 can be readily reduced at lower temperature due to their well mixed with CuO [33]. The real Fe_3O_4 in initial catalyst are different in some aspects from that formed in the reduction, such as the granularity of crystal, the dispersion, and the combination with promoters. They may exhibit different performance during pretreatment and FT reaction. The fact that the catalyst FO75 displayed lowest reduction temperature may correlate with its existence of highly dispersed of Fe_3O_4.

3.5. Reaction study in the fixed bed reactor

FT reaction tests in the fixed bed reactor were carried out under the conditions of 250 °C, 2.0 nL/g-cat/h, 1.5 MPa, and $H_2/CO = 2.0$. All the catalysts were stable during the 200 h of testing. Catalyst FO75 was the most active one with CO conversion around 75%. FO100 also had high CO conversion (>70%) within the reaction period. The activity of FO25 was moderate with CO conversion around 60%, while FO50 was very inactive with only around 25% CO conversion.

It has been demonstrated that the catalyst activity during FT synthesis is correlated with the formation of active phases. These active phases were formed both in activation process and in FT reaction. Previous XRD and MES studies display that catalyst FO100 has the highest amount of iron carbide after pretreatment, while FO50 has the lowest. Iron carbides have been supposed to be the most likely active phases in recent studies [19–21]. Although FO75 has much less iron carbides than FO100 after pretreatment, FO75 shows higher CO conversion. The amounts of iron carbides may be sufficient enough to provide FT active sites for both cases [34]. Other factors may exist during the process. First, Fe_3O_4 have been supposed to be the active phase for water-gas-shift (WGS) reaction for a long time [35]. Second, it was also found that Fe_3O_4 was correlated with the formation of iron carbides in recent studies [22,23]. In our XRD and MES experiments, FO25 and FO75 have much higher content of Fe_3O_4 in the catalyst samples after pretreatment, but the Fe_3O_4 phase in FO75 was well dispersed. It may be

partly evidenced from H_2-TPR that FO75 was as easily reduced as FO100, for the reason that the iron oxide in FO75 was well mixed with CuO promoter. After pretreatment, there is highly dispersed Fe_3O_4 formed in FO75 as well as iron carbides. From table 3, FO75 demonstrates highest WGS activity among all the four catalysts. It indicates that Fe_3O_4 in FO75 facilitate FT reaction by promoting the CO consumption. The initial Fe_3O_4 appeared to be inactive due to the fact that it is not highly dispersed and not well mixed with promoters such as CuO and K_2O. That may be the reason why FO50 was very inactive both in pretreatment and FTS.

From table 3 it can be seen that FO100 has the lowest methane selectivity (3.6 wt%) among the four catalysts, while FO50 has the highest, with CH_4 selectivity more than 6.8 wt%. Accordingly, FO100 favors hydrocarbon production of high molecular weight with C_5^+ selectivity of 81.3 wt%, while FO50 displays only 67.5 wt% of selectivity to C_5^+ hydrocarbons. As discussed above, catalyst FO75 shows a slightly higher CO conversion than FO100, but FO75 has higher methane selectivity and lower C_5^+ selectivity. This may be attributed to its high content of Fe_3O_4 in FO75, which promotes the WGS reaction (see table 3). Therefore, strong hydrogenation effect was observed. Especially lower selectivity to olefins for the catalyst supports the idea. It can be seen from table 3 that the ratio of olefin/paraffin (mole/mole) was 2.70 in C_5–C_{11} hydrocarbons and was 2.21 in C_{12}–C_{18} hydrocarbons for catalyst FO100. But the ratios were much lower for FO75, which was only 2.21 in C_5–C_{11} hydrocarbons and 0.60 in C_{12}–C_{18} hydrocarbons. This suggests a possibility that too much Fe_3O_4 in a working catalyst may correlate with higher hydrogenation effect, resulting in lower values of chain growth probability factor.

Other factors may have noticeable effect on activity and selectivity of the catalysts. For example, certain amount of sulfate in catalyst may improve its activity and modify the hydrocarbon selectivity [37], but too much of sulfate clearly poisons the catalyst [38]. Some promoter effects were also observed in our previous work when the sulfate content is less than 0.24 wt% compared to non-sulfate catalyst [25]. The fact that all the catalysts in this study have nearly the same contents of sulfate within the experimental error implies that sulfate impurity may impose the same effects on catalyst FTS performance. Moreover, the effects are most likely the positive ones for the catalyst group according to our previous work [24].

3.6. Reaction in a slurry reactor

In order to compare the long term FTS performance of the catalysts that have mixed iron phases with some commercial catalysts prepared from no-sulfate precursors, Catalyst FO100 was operated in a stirred tank slurry reactor (STSR) at 250 °C, 1.5 MPa, 2.0 nL/g-cat/h, and $H_2/CO = 0.67$ for 500 h. The detailed data of this test are listed in table 4, also with some literature results [36] for comparison. The catalyst was very active in its initial stage, with $(CO + H_2)$ conversion more than 77% before 200 h. Then, the catalyst deactivated gradually. The $(CO + H_2)$ conversion was 67% at the end of the test (500 h). The selectivity of CH_4 and C_{12}^+ for FO100 were 3.4 and 65.9 wt%, respectively. The results are comparable with Ruhrchemie (SB-2886) and Mobil (CT-256-13) catalysts, while the two catalysts were operated at higher temperature and lower space velocity.

The deactivation rate of the tested catalyst was 0.54%/day ($H_2 + CO$ conversion), which is higher than TAMU catalyst [36]. The activity loss may be ascribed to its high sodium content (see table 1), because sodium strongly facilitates the CO adsorption on catalyst surface, resulting in fast carbon deposition [39,40].

Table 3
Catalyst FTS performances in FBR

Reaction conditions	250 °C, 1.5 MPa, 2.0 nL/g-cat/h, $H_2/CO = 2.0$			
	FO25	FO50	FO75	FO100
Time on stream, h	60	72	54	72
CO conversion,%	60.7	25.5	75.0	70.6
$H_2 + CO$ conversion,%	35.2	17.4	48.9	41.7
WGS Kp (CO_2)[a]	7.7	3.1	12.5	9.9
FTS rate: k (mmol/g-cat./h/MPa)[a]	37.2	16.6	55.3	47.7
Hydrocarbon selectivities, wt%				
CH_4	5.0	6.8	5.5	3.6
C_2–C_4^0	6.1	8.4	6.5	4.5
C_2–$C_4^=$	13.4	17.3	12.6	10.6
C_5^+	75.5	67.5	75.4	81.3
$C_{5-11}^=/C_{5-11}$ (mol%)	2.61	2.67	2.21	2.70
$C_{12-18}^=/C_{12-18}$ (mol%)	1.12	1.08	0.60	1.10

[a]Based on the definitions in literature [36].

Table 4
Comparison of catalyst FTS performances in STSR

Catalyst Run ID	TAMU[a] SB-1931	Ruhrchemie[a] SB-2886	Mobil[a] CT-256–13	Cat-SP[b]	FO100
Reaction conditions					
Temperature (°C)	260	268	257	260	250
Pressure (MPa)	1.48	1.5	1.48	2.0	1.5
SV (nL/g-cat/h)	2.2–3.4	2.3	2.3	3.2	3.2
H2/CO	0.66–0.69	0.67	0.73	0.67	0.67
TOS (h)	40–520	215	457	115–550	500
(H2 + CO) conversion (mol%)	74–82	79	82	65–72	67–77
H2/CO Usage ratio	0.58–0.62		0.59	0.56–0.58	0.55–0.61
Hydrocarbon selectivities (*wt%*)					
CH4	3.0	6.4	2.7	2.8	3.4
C2–C4	10.5	18.2	11.1	13.9	13.3
C5–C11	16.0	27.2	18.1	24.3	17.4
C12+	70.5	48.2	68.1	59.0	65.9

[a]Data from literature [36].
[b]Data from our previous paper [24].

4. Conclusion

A series of $Fe/Cu/K/SiO_2$ catalysts for Fischer–Tropsch synthesis were prepared by a new method using iron sulfate precursors that have different oxidation state of irons. With the increase of initial oxidation degree of irons ($Fe^{3+}/Fe = 0.25$, 0.50, 0.75, and 1.0 theoretically), the BET surface areas and pore volumes of the as-prepared catalysts increase remarkably except for the catalyst with precursor of $Fe^{3+}/Fe = 0.50$ which is the lowest. XRD and MES results indicate that all the as-prepared catalysts are mixed iron oxides that have α-Fe_2O_3 (hematite) and Fe_3O_4 (magnetite) phases. As expected, the contents of α-Fe_2O_3 in the catalysts also increase following the original oxidation degree of irons except for the catalyst with precursor of $Fe^{3+}/Fe = 0.50$, while the content of Fe_3O_4 decrease following the same sequence. The XRD and MES studies for the catalysts samples after pretreatment show that Fe_3O_4 and iron carbides become the dominant phases. More iron carbides formed on the catalyst that has high content of α-Fe_2O_3 in its as-prepared state.

The FTS performance of the catalysts in FBR indicated that catalysts with precursor of $Fe^{3+}/Fe = 0.75$ and $Fe^{3+}/Fe = 1.0$ show the high FT activity with CO conversion more than 70% in 200 h of tests. Sufficient iron carbides may be associated with the improved FT activity. The role of Fe_3O_4 in the working catalysts, with the catalyst having precursor of $Fe^{3+}/Fe = 0.75$ as an example, may correlate with enhanced WGS activity when it was highly dispersed and well mixed with promoters such as CuO. High WGS activity results in promoted hydrogenation effects. This is partly responsible for its lower selectivity to olefin. Operation of the catalyst with precursor of $Fe^{3+}/Fe = 1.0$ in slurry reactor indicates that its FTS activity and selectivity are comparable with those reported in literatures.

Acknowledgments

We gratefully acknowledge financial support from The Key Engineering Projects of Chinese Academy of Sciences (KGCXI-SW-02) and "863" Project of Ministry of Science and Technology of China (2001AA523010).

References

[1] K. Jorthimurugesan, J.G. Goodwin, S.K. Gangwal and J.J. Spivey, Catal. Today 58 (2000) 335.
[2] R. Zhao, J.G. Goodwin, K. Jorthimurugesan, S.K. Gangwal and J.J. Spivey, Ind. Eng. Chem. Res. 40 (2001) 1065.
[3] Y. Jin and A.K. Datye, J. Catal. 196 (2000) 8.
[4] D.B. Bukur and C. Sivaraj, Appl. Catal. (A) 231 (2002) 201.
[5] D.B. Bukur, L. Nowichi and X. Lang, Chem. Eng. Sci. 49 (1994) 4615.
[6] M.E. Dry, in: *Catalysis Science and Technology*, Vol. 1, J.R. Anderson and M. Boudart (eds.), (Springer, New York, 1981)Chapter 4.
[7] B.H. Davis, Catal. Today 84 (2003) 83.
[8] D.B. Bukur, X. Lang, D. Mukesh, W.H. Zimmerman, M.P. Rosynek and C. Li, Ind. Eng. Chem. Res. 29 (1990) 1588.
[9] J.F. Shultz, W.K. Hall, T.A. Dubs and R.B. Anderson, J. Am. Chem. Soc. 28 (1956) 282.
[10] R. Dictor and A.T. Bell, J. Catal. 97 (1986) 121.
[11] K.R.P.M. Rao, F.E. Huggins, V. Mahajan, G.P. Huffman, V.U.S. Rao, B.L. Bhatt, B.D. Bukur, B.H. Davis and R.J. O'Brien, Top Catal. 2 (1995) 71.
[12] L.D. Mansker, Y. Jin, D.B. Bukur and A.K. datye, Appl. Catal. A 186 (1999) 277.
[13] J.P. Reymond, P. Meriaudeau and S.J. Teichner, J. Catal. 75 (1982) 39.
[14] C.S. Kuivila, P.C. Stair and J.B. Butt, J. Catal. 118 (1989) 299.
[15] D.J. Dwyer and G.A. Somorjai, J. Catal. 52 (1978) 291.
[16] C.S. Huang, L. Xu and B.H. Davis, Fuel Sci. Technol. Int. 11 (1993) 6.
[17] D.B. Bukur, X. Lang and Y. Ding, Appl. Catal. A (1999) 255.
[18] G. Bian, A. Oonnuki, N. Koizumi, H. Nomoto and M. Yamada, J. Mol. Catal. A 186 (2002) 203.
[19] K. Sudsakorn, J.G. Goodwin and A.A. Adeyiga, J. Catal. 213 (2003) 204.

[20] T.R. Motjope, H.T. Dlamini, G.R. Hearne and N.J. Coville, Catal. Today 71 (2002) 335.
[21] S. Li, G.D. Meitzner and E. Iglesia, J. Phys. Chem. B 105 (2001) 5743.
[22] S. Li, W. Ding, G.D. Meitzner and E. Iglesia, J. Phys. Chem. B 106 (2002) 85.
[23] S. Li, S. Krishnamoorthy, A. Li, G.D. Meitzner and E. Iglesia, J. Catal. 206 (2002) 202.
[24] B. Wu, L. Bai, H. Xiang, Y.W. Li, Z. Zhang and B. Zhong, Fuel 83 (2004) 205.
[25] B. Wu, L. Tian, L. Bai, Z. Zhang, H. Xiang and Y.W. Li, Catal. Comm. 5 (2004) 253.
[26] I. Tomoyuki, H. Nagata, O. Yamase, H. Matsuda, T. Kuroda, M. Yoshikawa, T. Takeguchi and A. Miyamoto, Appl. Catal. 24 (1986) 257.
[27] Y. Yang, H. Xiang, Y. Xu, L. Bai and W.Y. Li, Appl. Catal. A. 266 (2004) 181.
[28] D.B. Bukur, L. Nowichi, R.K. Manne and X. Lang, J. Catal. 155 (1995) 366.
[29] R. Fan, X.H. Chen, Z. Gui, L. Liu and Z.Y. Chen, Mater. Res. Bull. 36 (2001) 497.
[30] M.D. Shroff, D.S. Kalakkad, K.E. Coulter, S.D. coulter, M.S. Harrington, N.B. Jackson, A.G. Sault and A.K. Datye, J. Catal. 156 (1995) 185.
[31] N. Sirmanothan, H.H. Hamdeh, Y. Zhang and B.H. Davis, Catal. Lett. 82 (2002) 181.
[32] D.B. Bukur, K. Okabe, M.P. Rosynek, C. Li, D. Wang, K.R.P.M. Rao and G.P. Huffman, J. Catal. 155 (1995) 353.
[33] Y. Jin and A.K. Datye, J. Catal. 196 (2000) 8.
[34] K.R.P.M. Rao, F.E. Huggins, G.P. Huffman, R.J. Gormley, R.J. O'Brien and B.H. Davis, Energy Fuels 10 (1996) 546.
[35] G.P. Van der Laan and A.A.C.M. Beenackers, Catal. Rev. – Sci. Eng. 41 (1999) 255.
[36] D.B. Bukur, L. Nowichi and X. Lang, Chem. Eng. Sci. 49 (1994) 4615.
[37] W.L. Dijk, J.W. Niemantsverdriet, H.S. Van der Kraan and Van der Baan, Appl. Catal. 2 (1982) 273.
[38] T.C. Bromfield and N.J. Coville, Appl. Catal. A 186 (1999) 297.
[39] R.A. Diffenbach and D.J. Fauth, J. Catal. 100 (1986) 466.
[40] T.R. Motjope, H.T. Dlamini, G.R. Hearne and N.J. Coville, Catal. Today 71 (2002) 335.